MOLECULAR IMAGING AND BIOLOGY

World Molecular Imaging Society

RESEARCH ARTICLE

IND-Directed Safety and Biodistribution Study of Intravenously Injected Cetuximab-IRDye800 in Cynomolgus Macaques

Kurt R. Zinn,[1] Melissa Korb,[2] Sharon Samuel,[1] Jason M. Warram,[2] David Dion,[3] Cheryl Killingsworth,[5] Jinda Fan,[1] Trenton Schoeb,[4] Theresa V. Strong,[3] Eben L. Rosenthal[2]

[1]Department of Radiology, University of Alabama at Birmingham, Volker Hall G082, 1670 University Boulevard, Birmingham, AL, 35294, USA
[2]Department of Surgery, University of Alabama at Birmingham, Birmingham, AL, USA
[3]Department of Medicine, University of Alabama at Birmingham, Birmingham, AL, USA
[4]Department of Genetics, University of Alabama at Birmingham, Birmingham, AL, USA
[5]Animal Resources Program, University of Alabama at Birmingham, Birmingham, AL, USA

Abstract

Purpose: The use of receptor-targeted antibodies conjugated to fluorophores is actively being explored for real-time imaging of disease states; however, the toxicity of the bioconjugate has not been assessed in non-human primates.
Procedures: To this end, the *in vivo* toxicity and pharmacokinetics of IRDye800 conjugated to cetuximab (cetuximab-IRDye800; 21 mg/kg; equivalent to 250 mg/m^2 human dose) were assessed in male cynomolgus monkeys over 15 days following intravenous injection and compared with an unlabeled cetuximab-dosed control group.
Results: Cetuximab-IRDye800 was well tolerated. There were no infusion reactions, adverse clinical signs, mortality, weight loss, or clinical histopathology findings. The plasma half-life for the cetuximab-IRDye800 and cetuximab groups was equivalent (2.5 days). The total recovered cetuximab-IRDye800 in all tissues at study termination was estimated to be 12 % of the total dose. Both cetuximab-IRDye800 and cetuximab groups showed increased QTc after dosing. The QTc for the cetuximab-dosed group returned to baseline by day 15, while the QTc of the cetuximab-IRDye800 remained elevated compared to baseline.
Conclusion: IRDye800 in low molar ratios does not significantly impact cetuximab half-life or result in organ toxicity. These studies support careful cardiac monitoring (ECG) for human studies using fluorescent dyes.

Key words: Cetuximab, IRDye800, Toxicity, Macaques, Pharmacokinetics

Introduction

Near-infrared fluorophores have been developed for a variety of preclinical applications including the real-time, high-resolution imaging of labeled proteins. Fluorescent labeling can be used to improve and simplify assays designed to understand the fate of anticancer therapeutics after administration in humans. In addition to determining biodistribution, tissue penetration, and cellular localization, fluorescent-labeled therapeutics can also be used as companion diagnostics for accurate localization of cancer cells.

Furthermore, fluorescent-labeled proteins such as antibodies that specifically target cancer cells could be used for real-time cancer imaging during invasive procedures.

There are currently a growing number of fluorescent probes used for preclinical optical imaging and hardware designed around the emission and excitation wavelengths of these optical probes. IRDye800 was selected for the current study due to the reliable protein chemistry, high quantum yield, and good manufacturing practice (GMP) protocols used to produce the dye, making it ideal for human use. Furthermore, IRDye800 can be imaged using existing clinical imaging devices because the excitation and emission wavelengths are similar to indocyanine green which is widely used for diagnostic angiography in the clinic and operating room.

There are a growing number of antibody therapeutics that can be optically labeled for tissue and cellular localization. These antibodies can be used to image cancer in real-time to improve detection of subclinical disease during oncologic procedures. Unlike conventional anatomic imaging modalities including magnetic resonance imaging, X-ray computed tomography, and ultrasound—optical is better suited to intraoperative use because it can be used in real-time and can image in the surgical view (wide field imaging). Extensive preclinical work has been performed demonstrating that fluorescently labeled cetuximab is highly specific for cancer [1] and can detect microscopic fragments of tumor in flank and orthotopic models [2–7].

Cetuximab (ImClone LLC, a wholly owned subsidiary of Eli Lilly and Company, Branchburg, NJ) is a monoclonal antibody directed against the epidermal growth factor receptor (EGFR) that is overexpressed in a large number of cancers [8]. Because cetuximab is FDA-approved for colorectal cancer and head and neck cancer [9], repurposing this antibody from therapeutic agent to diagnostic agent can streamline clinical translation. Cynomolgus monkeys have historically been used in safety evaluation studies for cetuximab as they carry EGF receptors with a high degree of homology to humans.

The current study was performed to determine if IRDye800-labeled cetuximab would alter the pharmacokinetics and toxicity compared to unlabeled cetuximab. Specifically, the study aims were to evaluate the *in vivo* acute toxicity of cetuximab-IRDye800, compared with cetuximab, when administered via intravenous injection to cynomolgus monkeys; to study biodistribution at 15 days after dosing; to observe animals and determine acute (at 15 days) effects of the cetuximab-IRDye800; and to assess the location of the drug, persistence, or delayed occurrence of effects.

Methods

Cetuximab, IRDye800, and Conjugation

Cetuximab® antibody was supplied at 2 mg/ml. IRDye 800CW NHS ester (LI-COR Biosciences, Lincoln, NE) was supplied as a GMP-compliant reagent and was stored at ≤−70 °C prior to the conjugation. The fluorescent dye in this report is abbreviated as IRDye800. The University of Alabama at Birmingham (UAB) Vector Production Facility prepared the cetuximab-IRDye800 (lot UABVPF121114) under good laboratory practice (GLP) conditions, and the same lot was used for all animals in the cetuximab-IRDye800 treatment group. Cetuximab (lot IMF344, exp May 2015) for the cetuximab-dosed control group was obtained from the UAB pharmacy and stored in the Vector Production Facility in a monitored refrigerator. The same lot was used for all four animals in the cetuximab treatment group.

For the conjugation reaction, 400 mg of cetuximab was concentrated and pH adjusted by adding 10.5 ml of 1.0 M potassium phosphate, pH 8.9 (Acros Organics, Geel, Belgium) and exchanging buffer to potassium phosphate buffer, 50 mM, pH 8.5 using Amicon Ultra-15 devices (50,000 MWCO, EMD Millipore, Billerica, MA). After two rounds of concentrating and washing, a final solution of 10 mg/ml cetuximab in potassium phosphate buffer, 50 mM, pH 8.5, was achieved. The IRDye800CW NHS ester was hydrated in Water for Injection (WFI) at a concentration of 10 mg/ml; the dye and antibody were immediately mixed at a molar ratio of 2.3:1 and kept at 20 °C in the dark for 2 h. After 2 h, the cetuximab-IRDye800CW conjugation reaction mixture was layered onto phosphate buffered saline (PBS)-equilibrated Zeba Spin columns (4 ml/column), pH 7.4, and centrifuged at 2,100 rpm for 4 min to separate conjugate from free dye. The flow-throughs were pooled and the protein concentration adjusted with PBS to yield a concentration of 2 mg/ml. After filtration through a 0.22-μm polyvinylidene difluoride (PVDF) membrane, the IRDye800CW-conjugated cetuximab in PBS, pH 7.4, was vialed into 30-ml stoppered, evacuated vials (five vials at 25 ml each) and into 10-ml stoppered, evacuated vials (22 vials at 2.5 ml each) at a concentration of 2 mg of protein per ml and stored at 4 °C. Quality control testing on the final product included determination of the percent free by SDS-PAGE analysis; HPLC analysis; percent immunoreactivity as measured by binding to EGFR-coated beads; protein concentration; dye-to-protein ratio; pH; and safety testing including sterility, endotoxin, residuals, and bacteriostasis/fungistasis testing.

EGFR Immunoreactivity

Cetuximab/IRDye800 conjugates were assayed in triplicate for binding to EGFR-coated polystyrene beads. Briefly, biotinylated EGFR (EGR-H8222, ACROBiosystems, Newark, DE) at a concentration of 5.0 μg/ml in Dulbecco's phosphate buffered saline (DPBS), pH 7.0 with Ca^{2+} and Mg^{2+} (21-030-CV, Mediatech Inc., Manassas, VA), was immobilized to streptavidin-modified polystyrene beads (10041, Epitope Diagnostics, San Diego, CA). The excess EGFR was removed, and the beads were incubated in triplicate in 0.1 % bovine serum albumin (BSA) in DPBS pH 7.4 without Ca^{2+} and Mg^{2+} (Mediatech #21-031-CV) with and without cetuximab in excess. After 1 h, the solutions were removed from the beads, and cetuximab-IRDye800 conjugates, which had been diluted to 100 ng/ml with 0.1 % BSA in DPBS pH 7.4, were added. Triplicate aliquots (0.5 ml each) of cetuximab-IRDye800 were incubated with EGFR-coated beads, with and without blocking by 750 ng of unlabeled cetuximab. After 1 h room temperature incubation with gentle rocking, the supernatants were collected and the beads washed three times with DPBS, pH 7.4. The beads

(bound) and supernatants (unbound) were quantitatively imaged for fluorescence using a Pearl Impulse Imaging System (LI-COR, Lincoln, NE). The data were analyzed to determine the percentage of the sample bound to the EGFR-coated beads (emissions of the beads divided by the total emissions per reaction) and compared to a reference standard. Nonspecific binding when blocked by cetuximab was calculated as the emissions of the blocked beads divided by the total emissions of the blocked reaction. Specific binding was calculated as the percent of sample bound less the nonspecific binding divided by the percent of sample bound. Lot release specifications included a minimum of 90 % specific binding as well as total specific blocking greater than 85 % of that demonstrated by a reference standard.

Animals and Treatments

All animal experiments were reviewed and approved by the UAB Institutional Animal Care and Use Committee before they were started. Male cynomolgus macaques ($n=8$) were obtained from Covance Research Products (Denver, PA). Animals were approximately 3 years old at initiation of study. Weights ranged from 2.9 to 3.3 kg. Animals were fed Harlan Teklad Global 20 % Protein Primate biscuits (Harlan Laboratories, Tampa, FL) two times a day with six to eight biscuits provided for each feeding and were fed fresh produce (fruit or vegetable) once per day.

Animals were divided into two groups (four/group). One group was dosed with cetuximab-IRDye800 and the second group was dosed with cetuximab. One animal from each group was infused on each of the 4 days using an established procedure. All animals were dosed at 250 mg/m^2 (20.83 mg/kg), the full human therapeutic dose level of cetuximab. The study was terminated at 15 days (~4× biological half-lives) based on data indicating a blood half-life of 2.7 and 4 days for doses of 7.5 and 24 mg/kg in male cynomolgus macaques, respectively [10].

Animals were sedated with a combination of ketamine-dexdomitor given intramuscularly, intubated, and maintained under anesthesia on inhaled isoflurane delivered in oxygen. An intravenous catheter was placed in the cephalic vein and catheter site recorded. ECG data (surface leads I, II, and II) were collected immediately before test article infusion and every 10 min during the 1-h infusion. The doses were prepared and infused according to an established standard operating procedure. The infusions were accomplished with a Medfusion 3500 (M97327, Smiths Medical, Dublin, OH). Each animal was observed two to three times per day for mortality, appetite, abnormalities, and signs of pain or distress; findings were recorded as they were observed. At least three times during the pre-dose phase, before dosing on the day of treatment and at time of sacrifice, the animals were observed for weight gain or loss.

Animals were anesthetized with 2.0 mg/kg ketamine mixed with 50 µg/kg dexdomitor for all procedures other than infusions; during the same anesthesia procedure, the SPY Imaging, ECG, and blood collection were accomplished. Isoflurane anesthesia was used for infusions. Animal observations included imaging the animals with a SPY camera (Novadaq, Toronto, Canada). Images were collected before dosing $t_{initial}$ (initial), and after dosing at t_{1h}, t_{1d}, t_{3d}, t_{7d}, t_{10d}, and t_{15d} (before and after necropsy) for the group receiving cetuximab-IRDye800.

Hematology and Clinical Chemistry

Animals were fasted for sample collections. Blood samples were shipped by overnight delivery to Antech GLP (Morrisville, NC) on the day of collection. Blood samples from all animals were taken at least two times during the acclimation, pre-dose phase (>50 days) and at t_{3d} and t_{15d} after dosing. Blood analysis included a complete blood count with differential white cell count. Standard chemistries were sent including the following: blood urea nitrogen (BUN), total protein (TPROT), albumin (ALB), alanine aminotransferase (ALT), aspartate aminotransferase (AST), alkaline phosphatase (ALP), lactate dehydrogenase (LDH), creatine phosphokinase (CPK), gamma glutamyl transferase (GGT), cholesterol (CHOL), triglycerides (TRIG), total bilirubin (TBIL), troponin I (TRI): 16 samples only (all eight animals before treatment and all eight animals at 3 days after treatment), direct bilirubin (DBIL), electrolytes (Na, K, Cl), glucose (GLU), creatinine (CREA), ALP, calcium (CA), magnesium (MG), inorganic phosphorus (PHOS), amylase (AMY), lipase (LIP), prothrombin time (PT), and activated partial thromboplastin time (APTT). Blood samples (1.0 ml) from all animals were collected in a purple-topped Vacutainer (containing EDTA as an anticoagulant) prior to test article infusion $t_{initial}$ (initial), and after dosing at t_{1h}, t_{1d}, t_{3d}, t_{7d}, t_{10d}, and t_{15d}. Whole blood and plasma was frozen.

Cardiac and Respiratory Data Collections

For infusions, ECG data (surface leads I, II, and II) were collected immediately before test article (or cetuximab) infusion and every 10 min thereafter during the 1-h infusion. ECG data (surface leads I, II, and II) were also collected on at least three different days during the acclimation; pre-dose phase (>50 days); and at t_{3d}, t_{7d}, t_{10d}, and t_{15d} after dosing. Qtc: Surface electrograms were collected from the anesthetized animals. The uncorrected QT interval, R-R interval, heart rate as well as QT interval data corrected using Bazett's correction (called QTc=QT in msec/√R-R sec) were calculated on each electrocardiogram for all animals [11, 12]. Calipers were used to assess the raw data to determine all ECG intervals. Ten ECG complexes were measured at each time point and used in the analyses. Bazett's correction would not differ from Fridericia correction for our study, especially since heart rate did not differ for the two treatment groups [13]. Respirations per minute (RPM) were quantitated at the same time points.

Postmortem Procedures

The animals were euthanized via high anesthetic overdose of pentobarbital followed by exsanguination by severing the posterior humeral circumflex artery under each armpit. The necropsy included an examination of the external features of the carcass; external body orifices; the abdominal, thoracic, and cranial cavities; organs; and tissues. Table 1 lists tissues collected for routine analysis and routine histology, those in bold were weighed at necropsy. The liver and gallbladder were weighed together. The pituitary and prostate were collected for histology only, while all other tissues were collected for both histology and fluorescence analyses. When duplicate organs were present, the left sides were used for histology, while the right side was used for other measurements.

Table 1. List of tissues collected for whole-body biodistribution

Organ or tissue
1. Non-haired skin
2. Haired skin
3. Thyroid
4. *Heart*
5. *Lung*
6. Thymus
7. *Liver*
8. *Gallbladder*
9. *Spleen*
10. Pancreas
11. Mesenteric lymph node
12. Inguinal lymph node
13. Axillary lymph node
14. Stomach
15. Duodenum
16. Jejunum
17. Ileum
18. Cecum
19. Colon
20. Rectum
21. *Kidney, left*
22. *Kidney, right*
23. Adrenal glands
24. Bladder
25. Seminal vesicles
26. Prostate
27. *Testicle, right*
28. *Testicle, left*
29. Leg muscle
30. Femur (marrow)
31. Eye, left
32. Eye, right
33. Brain—cortex
34. Brain—cerebellum
35. Brain—midbrain
36. Pituitary
37. Spinal cord
38. Fat—omental
39. Fat—scalp
40. Nipple
41. Tissue under nipple
42. Tongue
43. Cheek mucosa
44. Lip
45. Trachea
46. larynx—vocal cords
47. Mandible
48. Salivary gland—submandibular

Organs in italics above were weighed during necropsy

Histopathology

The protocol-specified tissues from each animal were sectioned at approximately 5 μm, stained with hematoxylin-eosin (H&E), and reviewed by a veterinary pathologist (Trenton Schoeb, DVM, Ph.D., DACVP).

Animal Biodistribution

Biodistribution of the cetuximab-IRDye800 was determined at day 15 and compared with background autofluorescence from tissues collected from animals dosed with cetuximab. Cetuximab was not determined in these tissues (except for blood by Western blotting).

Blood and tissue samples were assayed for fluorescence with both groups of tissues in the same field of view, with standards also included. A standard curve (see inset Fig. 3) from fluorescence levels versus known levels of cetuximab-IRDye800 was used to convert the fluorescence levels in tissues to microgram of cetuximab-IRDye800, with normalization to weight of tissue measured (~50 mg) and to the total dose of cetuximab-IRDye800 (to yield %ID/g). The total microgram of cetuximab-IRDye800 in the total blood (μg total blood) was calculated by multiplying of the microgram per gram of blood by the total grams of blood (7 % of body weight). In the case of the blood, 1 g was 1 ml, as the blood was pipetted and not weighed for all measurements. Published values were used to determine the biodistribution [14–17]. In the case of non-haired and haired skin, both were estimated at 8 % of body weight for each of the skin samples (total 16 % estimate for skin); the muscles estimated at 40 % of body weight; the femur and mandible samples estimated at 7.5 % each (total 15 % estimate for skeleton); the brain was estimated at 2.35 % of body weight; and the intestines (stomach to rectum) were estimated at 7.6 % of body weight. The estimates for the brain and intestine were averages from a prior cynomolgus study at UAB with animals (n=9) of similar body size (3.2 kg), where these tissues were actually weighed at necropsy [18].

A range of concentrations of the cetuximab-IRDye800 was spiked to cynomolgus whole blood in the same geometry as the standards to investigate potential light attenuation by blood. It was found that the fluorescence signal recovered averaged 88 % (SD= 3.7 %), compared with the same levels of cetuximab-IRDye800 spiked in PBS. Since the tissues would contain 50 % or less of blood, and therefore have 6 % or less attenuation, it was decided not to correct the tissue data for blood presence.

Western Blotting of Plasma for Cetuximab and Cetuximab-IRDye800

Detection of cetuximab in the plasma was performed using Western blotting. Aliquots of plasma samples were mixed with 4X sample buffer and resolved by NuPAGE 4–12 % Bis-Tris gel (Invitrogen Corporation; Carlsbad, CA). Protein standards and a known amount of cetuximab-IRDye800 were loaded on each gel. The gel cassette was immediately imaged on the Pearl Impulse Imaging System using the 800-nm acquisition channel to verify cetuximab-IRDye at the 150-kDa marker. After imaging, the gel was electrophoretically transferred onto PVDF membrane (Millipore Corporation; Billerica, MA). Membranes were washed in TBS containing 5 % non-fat dry milk and 0.1 % Tween-20 for 1 h before adding 1:1,000 Goat anti-human IRDye 680RD (LI-COR Biosciences, Lincoln, NE) and incubated for an additional hour. The membranes were washed with three changes of TBS-T for 10 min each, wrapped in clear plastic, and imaged in the Pearl imager using the 700- and 800-nm channels for verification of cetuximab and cetuximab-IRDye800. Pearl software was used for analysis: regions of interest were drawn around the fluorescence signal (protein) as well as the bottom of the gel where the free dye (FD) was found. The signal was converted to microgram of cetuximab (or cetuximab-IRDye800) based on running known cetuximab standards and establishing a standard curve with the same software analyses as described. Percentage of fluorescence associated with the cetuximab band was determined by subtracting background from the band and dye front ROIs and using the background-corrected signals to determine (protein/FD+protein)×100 %.

Statistical Analyses

The statistical analyses were conducted using the Statistical Analyses System (SAS) program ver. 9.2. The general linear model (proc GLM) was used to conduct two-way analyses of variance (ANOVA).

Results

## Cetuximab-IRDye800 was Made Under GLP Conditions

The final product was clear, light green-blue liquid with no particulates, and has a dye/protein ratio of 1.8. There was 1.9 % free dye in the final product based on gel electrophoresis (data not shown). The immunoreactivity was not different from the reference standard using whole cell assays and ligand-based assays. The cetuximab-IRdye800 had greater than 90 % of binding to EGFR blocked by excess cetuximab, indicating the binding was specific. Endotoxin levels were less than 0.05 EU/ml.

Observation of Animals, Body Weights, and Histopathological Assessment

The clinical observations of the animals were normal throughout the experiment. There were no infusion reactions. The mean body weight of the cetuximab-IRDye800 and cetuximab groups increased during the measured time points. There were no histopathological findings attributable to cetuximab-IRDye800 or cetuximab.

Near-Infrared Imaging of Cetuximab-IRDye800 Infused Macaques

Near infrared imaging was performed with the SPY imaging system, which we have previously shown can be used to image antibody-IRDye800 bioconjugates [19]. In general, the surface vasculature was readily apparent after infusion of the cetuximab-IRDye800. Images of the thorax and abdomen had a homogenous and diffuse pattern of low-level fluorescence at each imaging point throughout the experiment; no deep tissues could be detected. Once the overlying tissues were removed at necropsy, the thymus, liver, and abdominal viscera had relatively high fluorescence and appeared distinctly brighter than their surrounding tissues. Veterinary staff discovered that one submissive animal had minor abrasions on the right eye and left first digit from a dominant male. The injuries to the eye (Fig. 1) and digit were noted to have increased uptake of cetuximab-IRDye800, with wound-to-background ratios (WBR) of 3.0 and 4.6, respectively. Background was measured from the adjacent skin. Over the course of the experiment, complete healing was noted and the fluorescence decreased considerably (see Fig. 1).

Day 1   Day 3   Day 7   Day 10
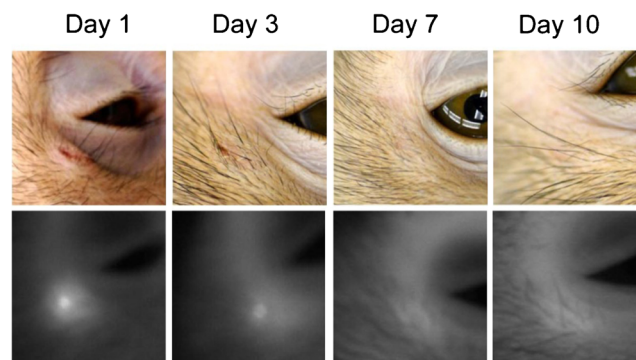
Fig. 1. Cetuximab-IRDye800 imaging in macaques. White light (*top*) and fluorescent images (*bottom*) are shown of minor abrasions on the right eye of individual macaque in the cetuximab-IRDye800 group. The injuries to the eye were noted to have increased uptake of cetuximab-IRDye800, which returned to baseline by day 10 post infusion.

Hematology and Chemistry Data

There were no statistically significant differences between the cetuximab and cetuximab-IRDye800 groups for the hematology parameters. There were also no significant differences between pretreatment and posttreatment for the cetuximab and cetuximab-IRDye800 groups. Clinical chemistry group averages were within normal ranges at all time points. Compared with pretreatment, after treatment, there were statistically significant ($p < 0.05$, using two-way ANOVA) increases in three enzyme parameters for both the cetuximab and cetuximab-IRDye800 groups, for ALT, AST, and LDH, respectively. There was no statistically significant difference between the cetuximab and the cetuximab-IRDye800 groups.

The CA level for the cetuximab group averaged 8.7 ± 0.2 mg/dL before treatment and was not statistically different ($p > 0.05$) than 9.2 ± 0.2 mg/dL after treatment. However, the CA level for the cetuximab-IRDye800 group averaged 8.74 ± 0.16 mg/dL before treatment and increased significantly ($p < 0.05$) to 9.32 ± 0.18 mg/dL after treatment. After treatment, there was no statistically significant difference between the cetuximab and the cetuximab-IRDye800 groups (9.2 ± 0.2 vs. 9.3 ± 0.2 mg/dL, respectively).

There was a statistically significant decrease ($p < 0.05$, two-way ANOVA) in BUN after treatment when both groups were combined, but it was not felt to be clinically relevant. There was no statistically significant difference between the cetuximab and the cetuximab-IRDye800 groups. Serum from all eight animals before treatment and at 3 days after treatment (~72 h) was tested for troponin I. All samples had levels below the detection limits of 0.2 ng/ml.

Cardiac and Respiratory Data

Using all measurements before treatment (base 1–4), the cardiac beats per minute (BPM) for the cetuximab-

IRDye800 and cetuximab groups averaged 118 ± 5 and 117 ± 5, respectively, and were not significantly different ($p>0.05$, two-way ANOVA). Similarly, using all measurements after treatment (days 3–15), the BPM for the cetuximab-IRDye800 and cetuximab groups averaged 91 ± 5 and 105 ± 5, respectively, and were not significantly different. However, for the cetuximab-IRDye800 group only (base 1–4 vs. Tx-Day3–15), the BPM before treatment at 118 ± 5 was significantly higher ($p<0.05$, two-way ANOVA) than the BPM after treatment at 91 ± 5. Within the cetuximab-IRDye800 group, the effect of treatment on BPM had resolved at day 15. There was no significant change in BPM during infusion for either group.

Using all measurements before treatment (base 1–4), the RPM for the cetuximab-IRDye800 and cetuximab groups averaged 48 and 59, respectively, and were not significantly different ($p>0.05$). Similarly, using all measurements after treatment (days 3–15), the RPM for the cetuximab-IRDye800 and cetuximab groups averaged 39 and 51, respectively, and were not significantly different. There was no significant change in respiration rate during infusion for either group ($p>0.05$).

Using all measurements before treatment (Fig. 2a: base 1–4), the QTc for the cetuximab-IRDye800 and cetuximab groups averaged 360 ± 2 and 364 ± 2 msec, respectively, and were not significantly different from each other ($p>0.05$). Similarly, using all measurements after treatment (Fig, 2a: Tx-Day3–15), the QTc for the cetuximab-IRDye800 and cetuximab groups averaged 379 ± 2 msec and 370 ± 2, msec, respectively, and were significantly different ($p<0.05$) from each other and from pretreatment levels. For the cetuximab-IRDye800 and cetuximab groups at days 3, 7, and 10 after treatment, the QTc means were significantly higher ($p<0.05$) than the means before treatment. Within the cetuximab treatment group only, the increase in QTc above baseline values after treatment had resolved by day 15 after treatment, and at day 15, the QTc was not different than baselines values ($p>0.05$). However, within the cetuximab-IRDye800 treatment group, the increase in QTc above baseline values after treatment had not resolved by day 15 after treatment, and at day 15, the QTc (371 msec) remained significantly higher ($p<0.05$) than baseline (360 msec) (Fig. 2a).

ECG monitoring was done on all animals immediately before and during infusions. When all data after infusion started (10–60 min) were compared with baseline before starting infusion, an overall significant increase in mean QTc during infusion was not found for the cetuximab-IRDye800 or the cetuximab groups ($p>0.05$, two-way ANOVA, Fig. 2b).

Whole-Body Biodistribution of Infused Macaques

The mean biodistribution data for cetuximab-IRDye800 and background fluorescence are presented in Figs. 3 and 4 as percent-injected dose per gram of tissue and estimated total microgram of the antibody bioconjugate in selected tissues,
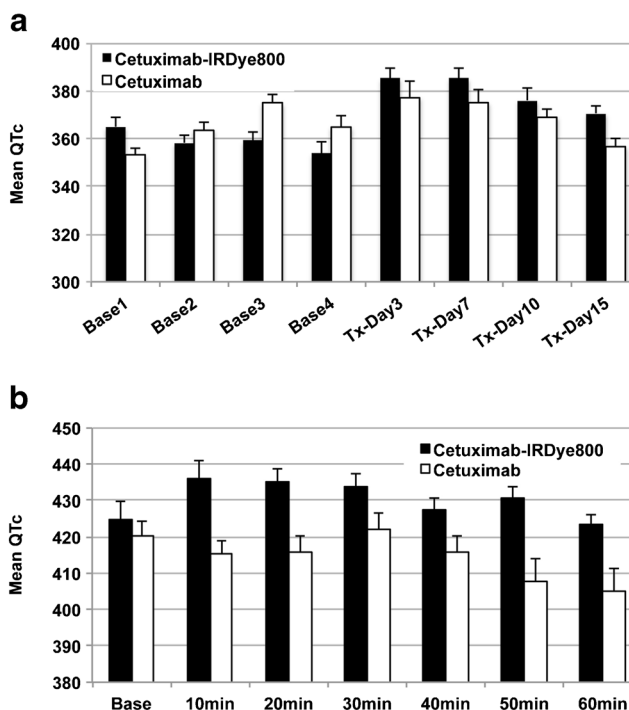
Fig. 2. **a** Corrected QTc before and after treatment. ECG data (surface leads I, II, and II) was collected on cetuximab and cetuximab-IRDye800 groups at three different days during acclimation (*Base 1–3*), pre-dose phase (*Base 4*), day 3 post infusion (*Tx-Day3*), day 7 post infusion (*Tx-Day7*), day 10 post infusion (*Tx-Day10*), and day 15 post infusion (*Tx-Day15*). QT interval data corrected using Bazett's correction (called QTc=QT in msec/√R-R sec) was calculated on each electrocardiogram for all animals. **b** Corrected QTc during infusion. QT interval data corrected using Bazett's correction (called QTc=QT in msec/√R-R sec) was calculated on each electrocardiogram for all animals at pre-dose (*Base*) and every 10 min during the 1-h infusion of cetuximab or cetuximab-IRDye800 groups. Values are mean QTc values± standard error.

respectively. A standard curve is included in Fig. 3; tissues were measured in the linear region. The cetuximab-IRDye800 could be accurately quantitated within tissues based on the localization of the IRDye800 by fluorescence and the total amount of dye estimated by extrapolating from organ necropsy data. As shown in Fig. 4, the total recovered cetuximab-IRDye800 in all tissues was estimated to be 8,903 µg, or 11.9 % of the total mean dose (63,700 µg), not corrected for background autofluorescence. The total background arising from autofluorescence in all tissues was estimated at 1,312 µg.

Pharmacokinetics of Cetuximab and Cetuximab-IRDye800

The mean levels of cetuximab-IRDye800 and cetuximab were measured in plasma over time, as determined by Western blotting (Fig. 5a and b). Importantly, there was no difference in
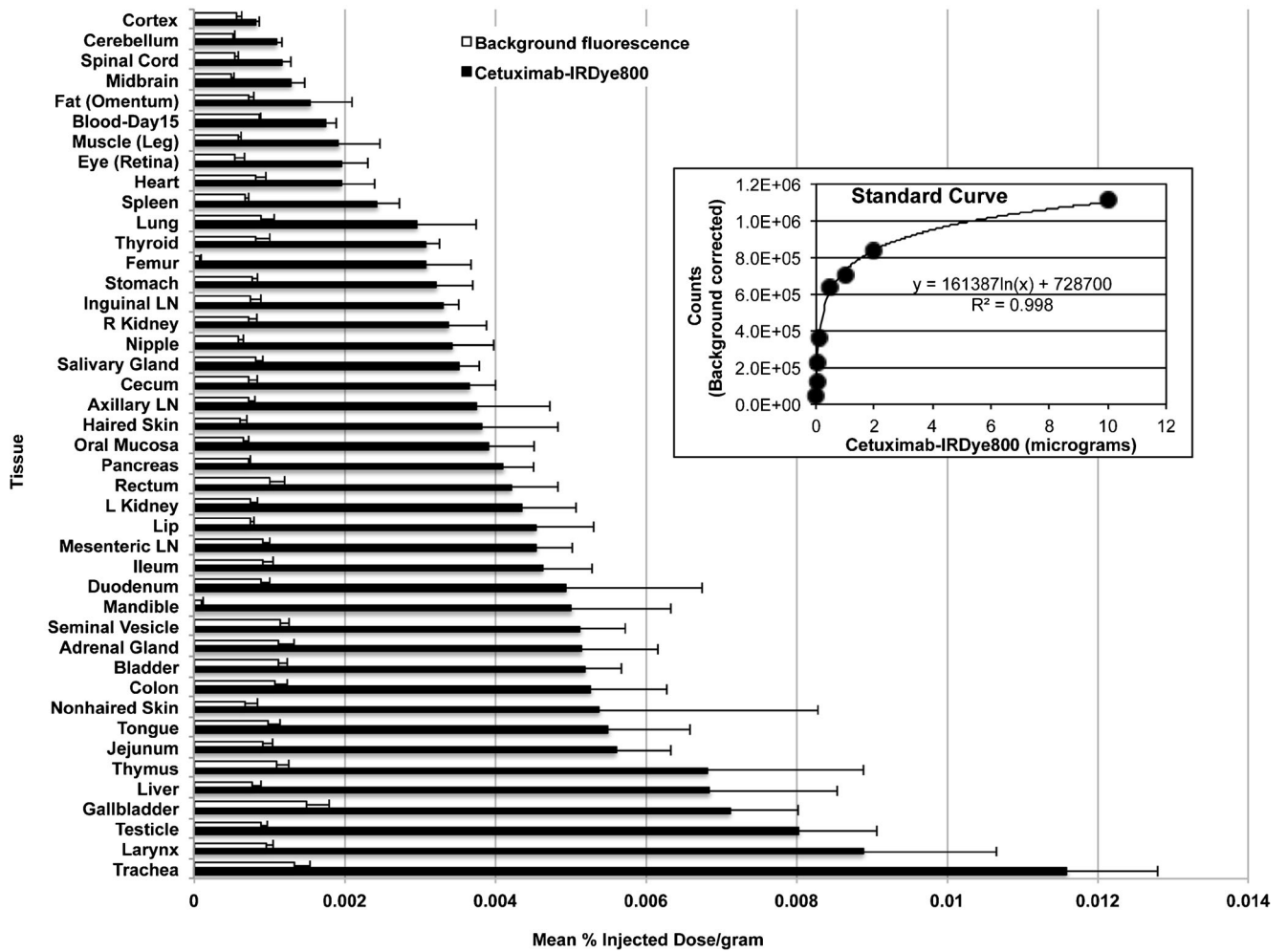
Fig. 3. Biodistribution in tissues. Background fluorescence and cetuximab-IRDye800 fluorescence is reported for all organs collected during whole-body biodistribution at day 15 post infusion. *Inset graph* shows a standard curve from fluorescence levels versus known levels of cetuximab-IRDye800. Values are reported as percent-injected dose (%ID) per gram of tissue± standard error.
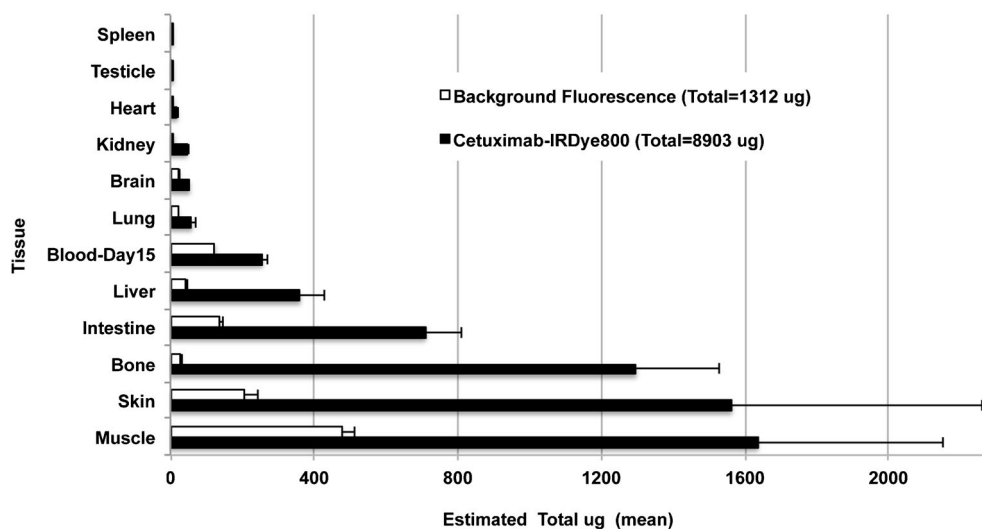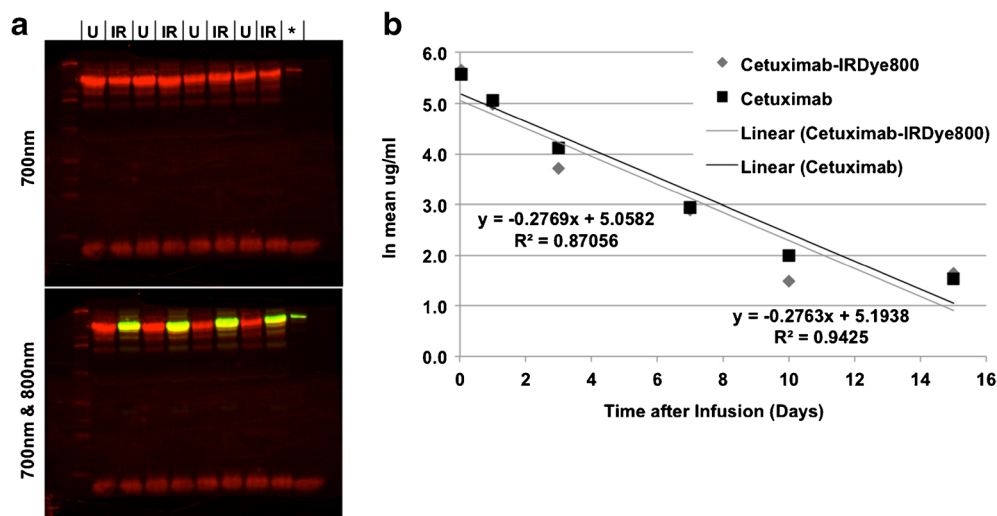

Fig. 4. Estimated total micrograms (μg) of cetuximab-IRDye800 in selected tissues. Background fluorescence and cetuximab-IRDye800 fluorescence is reported for selected tissues collected during whole-body biodistribution at day 15 post infusion. Values are reported as estimated total μg (mean)±standard error.

Fig. 5. Cetuximab and cetuximab-IRDye800 (mean μg ml) in the plasma over time as determined by Western blotting. **a** Panels show immunoblot of blood plasma from individual macaques (*n*=4) in the cetuximab-unlabelled group (*U*) and macaques (*n*=4) in the cetuximab-IRdye800 group (*IR*) imaged. A known amount of cetuximab-IRDye800 was also included (*asterisk*). In the *upper panel*, bands represent the presence of goat anti-human IRDye 680RD detected at the 150-kDa marker during Pearl Impulse acquisition of the membrane at the 700-nm channel. *Lower panel* shows fused image of Pearl Impulse acquisition using the 700- and 800-nm acquisition channel to verify cetuximab-IRDye800 at the 150-kDa marker. **b** A plot of the natural log of the mean blood level versus time yielded a line with a slope equal to −*k* and with the half-life equal to the Ln 2 divided by *k*. Values are mean micrograms per milliliter±standard error.

the clearance between the cetuximab-IRDye800 and cetuximab. A plot of the natural log of the mean blood level versus time yielded a line with a slope equal to −*k* and with the half-life equal to the Ln 2 divided by *k*. The half-life for the cetuximab-IRDye800 and cetuximab groups were not different, both having a value of 2.51 days. Western blotting demonstrated that the antibody-dye bioconjugate remained bound to each other with very limited free IRDye800 in the plasma after dosing until day 10.

Discussion

FDA-approved, therapeutic antibodies can be repurposed for image-guided diagnostics by the addition of a fluorescent dye. Identification of a fluorescent dye that can be used to label the rapidly expanding portfolio of antibody-based therapeutics, without added toxicity or significantly altering the immunoreactivity or antibody half-life, would permit the development of novel cancer-specific imaging opportunities and development of companion diagnostics. Previous toxicology studies in rodents using the carboxylate version of the IRDye800 alone did not demonstrate any significant toxicity despite very high dosing [20]. This is the first study to assess the safety and toxicity of an IRDye800-conjugated antibody.

The present study demonstrated cetuximab-IRDye800 to be well tolerated under the conditions of the study. There were no infusion reactions, adverse clinical signs, mortality, weight loss, or clinical histopathology findings. All statistically significant treatment effects were due to cetuximab and

not the IRDye800, with one exception discussed in the next paragraph.

Both cetuximab and cetuximab-IRDye800 increased QTc after dosing. The QTc for the cetuximab group returned to baseline levels at day 15, while the cetuximab-IRDye800 group remained elevated at day 15. This small but statistically significant difference in the QTc interval in the cetuximab-IRDye800 group was deemed to be important considering a prolonged QTc interval is associated with an eightfold higher risk of sudden cardiac death [21]. This information led to changes in our clinical trial assessing cetuximab-IRDye800 as an intraoperative imaging agent in head and neck cancer (clinical trials.gov NCT01987375). The trial was changed to include ECG monitoring for changes in QT interval and to exclude patients with known prolonged QT intervals, low blood Ca, or low blood Mg.

The current study cannot determine the clinical relevance in humans of the prolonged QTc in the cetuximab-IRDye800 group compared to the cetuximab group. FDA guidance documents require ECG monitoring to be capable of detecting increases of 5 msec in the QT interval. The QTc increase in this cynomolgus study was above that level, and therefore, ECG monitoring in the human study was necessary. The dose of cetuximab-IRDye800 to the macaques was fourfold higher than the highest dose for the human study. The highest dose level for the human study may not be necessary based on initial testing during surgery, and therefore, cardiac risk may be further reduced because the dose of cetuximab-IRDye800 would be reduced. In

addition, if successful for improving surgical resection of cancer, the cetuximab-IRDye800 would be administered just one time while cetuximab for therapy is given repeatedly over an extended period.

These results support the use of IRDye800 bioconjugates for clinical application, which has several important advantages. Firstly, clinical devices designed to image indocyanine green can be used to detect IRDye800. In addition, the dye is currently manufactured under GMP conditions suitable for human injection and has a significantly higher quantum yield compared to indocyanine green. In fact, these characteristics have made IRDye800 widely used in several clinical trials in Europe (clinical trials.gov NCT01972373; NCT01508572). However, these human trials are using antibody-dye bioconjugates at the microdose level (1/100th of therapeutic dose) and therefore underwent less-rigorous safety testing as part of the regulatory approval process. In the current study, we delivered the full therapeutic dose of cetuximab and cetuximab-IRDye800 with the understanding that diagnostic indications would most likely use doses well below the therapeutic level.

The IRDye800 could be accurately quantitated within tissues. For determining the levels of cetuximab-IRDye800 in the tissues (compared to the infused dose), it was assumed that the cetuximab-IRDye800 conjugate remained intact, and therefore, IRDye800 was a measurement of IRDye800-bound cetuximab. Based on this assumption, the total recovered cetuximab-IRDye800 in all tissues at day 15 was estimated to be 8,903 µg or approximately 12 % of the total mean dose. This estimate suggests a mean whole-animal half-life of 4.7 days. The background arising from autofluorescence of all tissues was 1,312 µg, as determined with measurements of all tissues from the cetuximab group. For the cetuximab-IRDye800 estimate (8,903 µg), the background (1,312 µg) was not subtracted.

Conclusion

The present study suggests that antibody-IRDye800, with appropriate cardiac monitoring, can be safely translated to the clinic for companion diagnostic imaging as well as image-guided oncologic surgery. There is a significant debate over which is the best cancer-targeting antibody based on a variety of parameters including signal-to-noise background, serum half-life, and safety. These scientific arguments favoring one cancer-targeting agent over another are somewhat muddled in preclinical debates that are subject to industry or intellectual property considerations [22]. Regardless of the protein selected for cancer- or disease-specific targeting, this data suggests large proteins can be safely labeled and administered to humans at doses above the microdose level.

References

1. Rosenthal EL, Kulbersh BD, Duncan RD et al (2006) In vivo detection of head and neck cancer orthotopic xenografts by immunofluorescence. Laryngoscope 116:1636–1641
2. Gleysteen JP, Duncan RD, Magnuson JS et al (2007) Fluorescently labeled cetuximab to evaluate head and neck cancer response to treatment. Cancer Biol Ther 6:1181–1185
3. Gleysteen JP, Newman JR, Chhieng D et al (2008) Fluorescent labeled anti-EGFR antibody for identification of regional and distant metastasis in a preclinical xenograft model. Head Neck 30:782–789
4. Kulbersh BD, Duncan RD, Magnuson JS et al (2007) Sensitivity and specificity of fluorescent immunoguided neoplasm detection in head and neck cancer xenografts. Arch Otolaryngol Head Neck Surg 133:511–515
5. Newman JR, Gleysteen JP, Baranano CF et al (2008) Stereomicroscopic fluorescence imaging of head and neck cancer xenografts targeting CD147. Cancer Biol Ther 7:1063–1070
6. Rosenthal EL, Kulbersh BD, King T et al (2007) Use of fluorescent labeled anti-epidermal growth factor receptor antibody to image head and neck squamous cell carcinoma xenografts. Mol Cancer Ther 6:1230–1238
7. Withrow KP, Newman JR, Skipper JB et al (2008) Assessment of bevacizumab conjugated to Cy5.5 for detection of head and neck cancer xenografts. Technol Cancer Res Treat 7:61–66
8. Rogers SJ, Harrington KJ, Rhys-Evans P et al (2005) Biological significance of c-erbB family oncogenes in head and neck cancer. Cancer Metastasis Rev 24:47–69
9. Giusti RM, Shastri KA, Cohen MH et al (2007) FDA drug approval summary: panitumumab (Vectibix). Oncologist 12:577–583
10. (2004) European public assessment report for Erbitux. Canary Wharf, London UK: European Medicines Agency
11. Joers V, Seneczko K, Goecks NC et al (2012) Nonuniform cardiac denervation observed by 11C-meta-hydroxyephedrine PET in 6-OHDA-treated monkeys. PLoS ONE 7:e35371
12. Regan CP, Stump GL, Wallace AA et al (2007) In vivo cardiac electrophysiologic and antiarrhythmic effects of an isoquinoline IKur blocker, ISQ-1, in rat, dog, and nonhuman primate. J Cardiovasc Pharmacol 49:236–245
13. Indik JH, Pearson EC, Fried K, Woosley RL (2006) Bazett and Fridericia QT correction formulas interfere with measurement of drug-induced changes in QT interval. Heart Rhythm 3:1003–1007
14. Alberts BJA, Lewis J (2002) Molecular biology of the cell. Garland Science, New York
15. Ross MHKG, Pawlina W (2003) Histology: a text and atlas. Lippincott Williams & Wilkins, New York
16. Spelke E (1994) Anatomy and physiology: an easy learner. Jones and Bartlett Publishers Inc., Burlington
17. En M (1989) Human anatomy and physiology. Benjamin/Cummings Publishing Company Inc., San Francisco
18. Kim H, Chaudhuri TR, Buchsbaum DJ et al (2007) High-resolution single-photon emission computed tomography and X-ray computed tomography imaging of Tc-99m-labeled anti-DR5 antibody in breast tumor xenografts. Mol Cancer Ther 6:866–875
19. Heath CH, Deep NL, Sweeny L et al (2012) Use of panitumumab-IRDye800 to image microscopic head and neck cancer in an orthotopic surgical model. Ann Surg Oncol 19:3879–3887
20. Marshall MV, Draney D, Sevick-Muraca EM, Olive DM (2010) Single-dose intravenous toxicity study of IRDye 800CW in Sprague-Dawley rats. Mol Imaging Biol 12:583–594
21. Straus SM, Kors JA, De Bruin ML et al (2006) Prolonged QTc interval and risk of sudden cardiac death in a population of older adults. J Am Coll Cardiol 47:362–367
22. Rosenthal EL (2014) Optical imaging of head and neck cancer: opportunities and challenges. JAMA Otolaryngol Head Neck Surg 140:93–94